Development of a Molecular Dynamics Method with Heat Transfer into Bulk for Ion Injection into Materials*)

Seiki SAITO, Hiroaki NAKAMURA[1,2)], Keiji SAWADA[3)], Masahiro KOBAYASHI[1,4)], Kawamura GAKUSHI[1,4)] and Hasuo MASAHIRO[5)]

Yamagata University, Yonezawa 992-8510, Japan
[1)]*National Institute for Fusion Science, Toki 509-5292, Japan*
[2)]*Nagoya University, Nagoya 464-8603, Japan*
[3)]*Shinshu University, Nagano 380-8553, Japan*
[4)]*The Graduate University for Advanced Studies, SOKENDAI, Toki 509-5292, Japan*
[5)]*Kyoto University, Kyoto 615-8540, Japan*

(Received 29 November 2019 / Accepted 13 July 2020)

When an ion or atom is injected into a target material, the incident energy increases the temperature around the injection point. Owing to the energy transfer to the surrounding atoms, the temperature of the material recovers to the initial temperature in the real system because heat is transferred to the bulk of material which consists of an almost infinite number of atoms. However, if we simulate the system by the molecular dynamics (MD) method, it is difficult to prepare a sufficiently large system to calculate the process of heat transfer to the bulk. Therefore, in this study, we develop an MD simulation model which includes the effect of heat transfer to the bulk by solving heat conduction equation. The simulation result shows that the process of heat removal proceeds on a time scale of approximately 1000 times slower than the time scale of the incident energy transfer from the incident atom to the target material.

Keywords: heat conduction, molecular dynamics, plasma material interaction, hydrogen, carbon, divertor, recycling

DOI: 10.1585/pfr.15.2403073

1. Introduction

The carbon divertor is bombarded by energetic hydrogen plasma in Large Helical Device (LHD) in National Institute for Fusion Science, Japan. When hydrogen ions irradiated divertor plates, some hydrogen atoms reflect back to the plasma, while other hydrogen atoms retain in the divertor. Investigating the recycling of hydrogen ions at the divertor is an important issue because these recycled hydrogen atoms or molecules affect [1] plasma parameters by charge exchange recombination and dissociative recombination. Information on recycled hydrogen atoms and molecules can be used for neutral-transport simulation [2, 3].

Molecular dynamics (MD) simulation allows simulating the particle injection process on an atomic scale. Our group plans to perform an MD simulation of a hydrogen atom injection into carbon materials to investigate the energy distribution of recycled atoms and molecules [4, 5]. Material temperature considerably affects the emission process of hydrogen atoms and molecules. Therefore, for this MD simulation, it is necessary to consider the process of heat transfer from the incident atom toward the surrounding atoms. Because thermal energy propagates to the surrounding atoms one after another, if the MD calculation with a sufficiently large number of atoms is performed, the elevation of the system temperature owing to the injection of one atom is not significant after the system reaches thermal equilibrium. However, owing to the computation cost, it is difficult to prepare a sufficiently large system to calculate the process of heat transfer to the bulk which is caused by the kinetic energy entering the target material with injected atoms. To avoid this problem, it is necessary to develop a calculation method that allows heat to escape from the MD system that consists of limited number of atoms.

When it is necessary to keep the temperature in the system constant, MD simulation, in most cases, is performed under the NVT ensemble, in which the number of particles (N), volume (V), and temperature (T) are conserved. However, the NVT ensemble is not applicable in our simulation because the collision process between incident and target atoms is a nonequilibrium process. Therefore, in this study, we propose a method to solve the thermal process of heat escaping outside the MD system by connecting the MD system to the heat conduction (HC) equation. In this method, the MD system is embedded in a larger system where HC is solved. The incident energy carried to the MD system by the injection of atoms is con-

author's e-mail: saitos@yz.yamagata-u.ac.jp
*) This article is based on the presentation at the 28th International Toki Conference on Plasma and Fusion Research (ITC28).

verted into thermal energy by collision with the surrounding atoms in the MD system and transferred outside the MD system.

2. Simulation Model and Method

2.1 MD simulation model

As shown in Fig. 1, a 40 Å × 40 Å × 33.3 Å hydrogen-contained amorphous carbon material is prepared as the target material. The target material consists of 3872 carbon and 2080 hydrogen atoms. The density of the carbon atoms is determined by MD simulation [6] by depositing the carbon atoms on a diamond substrate. The hydrogen concentration H/C is determined in the range of values obtained in the experiment [7].

An incident hydrogen atom is placed at a height of 10 Å from the surface of the target material. The x- and y-coordinates of the starting position of the incident hydrogen atom are set to the center of the target material. The incident energy is set to 100 eV. The incident angle is set to be parallel to the z-axis. For this incident energy, the incident atom reaches the surface of the target material 7.2 fs after the simulation started. The simulation time is set to 200 ps. The initial temperature of the target material is set to 300 K.

For atomic interactions, a modified reactive empirical bond order (REBO) potential [8] is employed as the potential function U. A carbon atom has four valence electrons and consequently, four (or fewer) covalent bonds. The potential function strongly depends on the bonding state of the carbon atom. The REBO potential is defined as follows:

$$U \equiv \sum_{i,j>i} \left[V^{\mathrm{R}}_{[ij]}(r_{ij}) - \bar{b}_{ij}(\{r\}, \{\theta^{\mathrm{B}}\}, \{\theta^{\mathrm{DH}}\}) V^{\mathrm{A}}_{[ij]}(r_{ij}) \right], \tag{1}$$

where r_{ij} is the distance between the i-th and the j-th atoms. Functions $V^{\mathrm{R}}_{[ij]}$ and $V^{\mathrm{A}}_{[ij]}$ represent repulsion and attraction, respectively. Function $\bar{b}_{ij}$ generates a multi-body force. The bond angle $\theta^{\mathrm{B}}_{jik}$ is an angle between the vector from the i-th atom to the j-th atom and the vector from the i-th atom to the k-th atom. The dihedral angle $\theta^{\mathrm{DH}}_{kijl}$ is the angle between the plane passing through the k-th, i-th, and j-th atoms and the plane passing through the i-th, j-th, and l-th atoms. Moreover, the parameters $\{r\}$, $\{\theta^{\mathrm{B}}\}$, $\{\theta^{\mathrm{DH}}\}$ denote the sets of r_{ij}, $\theta^{\mathrm{B}}_{jik}$, $\theta^{\mathrm{DH}}_{kijl}$, respectively.

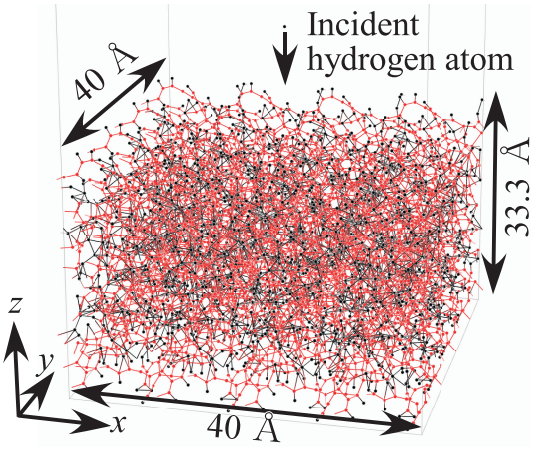

Fig. 1 System of the MD region. Red and black balls denote carbon and hydrogen atoms, respectively.

The motion of atoms (except in the connection cells, which will be explained later) is calculated under NVE ensemble, in which the number of particles (N), volume (V), and total energy (T) are conserved. A periodic boundary condition is used in the x- and y-directions. A second-order symplectic integration [9] is used to execute the time integration of the equation of motion. The time step Δt of the integration is set to 0.02 fs.

In this study, the average kinetic energy T^* of a certain region expressed in the unit of temperature is defined as the following equation:

$$T^* \equiv \left(\sum_i^N \frac{1}{2} m_i v_i^2 \right) \Big/ \left(\frac{3}{2} k_{\mathrm{B}} N \right), \tag{2}$$

where m_i and v_i are the mass and velocity of i-th atom, respectively. N is the number of atoms in the region. k_{B} is the Boltzmann constant. T^* expresses the temperature of the region when the atoms in the region are in thermal equilibrium.

2.2 Connection of MD simulation and HC equation

Because the incident hydrogen atom brings its kinetic energy into the target material, the thermal energy of target material increases at the injection. In a real system, the thermal energy gradually decreases by heat transfer toward the surrounding atoms. However, because of its long computation time, it is difficult to prepare an MD system that is sufficiently large to calculate the process of heat transfer to the bulk. To consider this heat transfer, we developed an MD-HC hybrid simulation, which is connects the MD method to the HC equation and expresses the heat transfer to the bulk.

Figure 2 shows the schematic diagram of the MD-HC hybrid simulation. Our system consists of both the molecular dynamics calculation region (MD region) and the heat conduction calculation region (HC region). To calculate the heat transfer flowing out from the MD region, the MD region is embedded in the HC region. The entire system, include the MD and HC region, is divided into 6.67 Å × 6.67 Å × 6.67 Å cells. The total number of cells is set to 26 × 26 × 26. As shown in Fig. 3, the MD and HC region are connected by the connection cells. Connection cells are also shown as hatched cells in Fig. 2. The number of cells in the MD region, including connection cells, is 6 × 6 × 5.

To calculate the HC equation, each cell stores the value of T_{cell}, which is the temperature of the cell. The

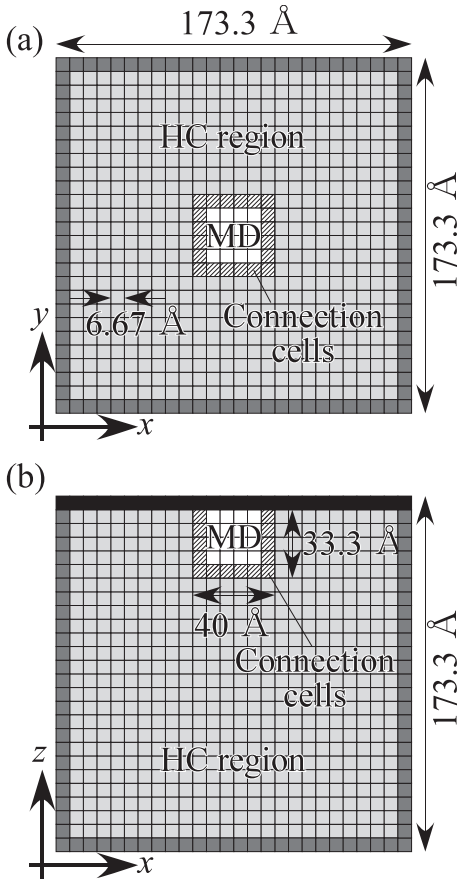

Fig. 2 Cross-sectional schematic diagram in the (a) x-y and (b) x-z planes of the system of the MD-HC hybrid simulation, which consists of the MD and HC regions.

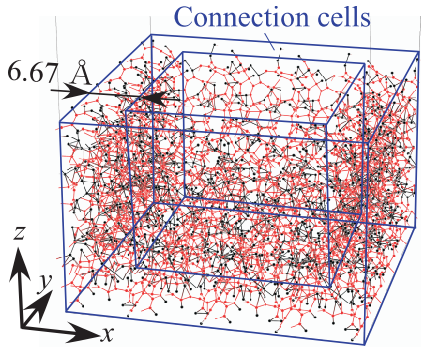

Fig. 3 Atoms in the connection cells. The red and black balls denote carbon and hydrogen atoms, respectively.

value of T_{cell} in the MD region is calculated using Eq. (2) although it is not possible to assume that some cells in the MD region are in thermal equilibrium. The time evolution of T_{cell} is solved using the following HC equation:

$$\frac{\partial T_{\mathrm{cell}}}{\partial t} = \alpha \nabla^2 T_{\mathrm{cell}}, \tag{3}$$

where α is the thermal diffusivity. The cells shown in dark gray in Fig. 2 are used for the Dirichlet boundary condition by fixing the temperature T_{cell} to the bulk temperature 300 K. The cells shown in black in Fig. 2 are used for the Neumann boundary condition by copying the T_{cell} value of the cell located one cell below in the z-axis direction.

The time step Δt of the integration is set to 0.02 fs, which is the same value used in the MD simulation. Of note, the time scale of most HC phenomena is slower than that of atomic motion in the MD system. Therefore, it is possible to use a longer time step for HC calculation than for MD calculation. However, because of the computation cost for HC calculation is negligibly small compared with the computation cost for the MD system, the same value is used for the time step of the MD and the HC calculation in our simulation.

The time evolution of the system is calculated using the following procedure:

1. The momentums of atoms in the MD region are determined to follow the Maxwell-Boltzmann distribution with an initial temperature of 300 K.
2. T_{cell} for all cells is set to 300 K.
3. The momentums of atoms in the MD region are proceeded by $\Delta t/2$.
4. The positions of atoms in the MD region are proceeded by $\Delta t/2$.
5. The force acting on all atoms in the MD region is updated.
6. The T^* values of each cell in the MD region, including connection cells, are calculated by Eq. (2).
7. The T_{cell} values of each cell in MD region, including connection cells, are overwritten with the calculated value of T^*.
8. The T_{cell} values of cells in the HC region and connection cells are proceed by Δt. (The T_{cell} of other cells in the MD region do not have to be proceeded.)
9. The momentums $\boldsymbol{p}$ of atoms in the MD region are updated to $\boldsymbol{p}'$ using the velocity scaling method:
$$\boldsymbol{p}'_i = \boldsymbol{p}_i \sqrt{T_{\mathrm{cell},i}/T_i^*},$$
where $\boldsymbol{p}_i$ is the momentum of the i-th atom before the update. $T_{\mathrm{cell},i}$ and T_i^* are the values of T_{cell} and T^* of the cell to which the i-th atom belongs.
10. Repeat steps 3 to 9.

2.3 Determination of thermal diffusivity α

To obtain the thermal diffusivity α of the target material shown in Fig. 1, another MD simulation shown in Fig. 4 (a) is performed. In the MD simulation, a 10 Å × 10 Å × 200 Å hydrogen-containing amorphous carbon material is prepared in the simulation box. The densities of hydrogen and carbon atoms in this simulation are set to the same density of the target material used for the injection simulation shown in Fig. 1. Then, the time evolution of HC is investigated by heating one end. A periodic boundary condition is used in the direction perpendicular to the depth direction while open boundary is applied in the depth direction. To heat one end, the initial velocities of atoms

within 10 Å from the edge of the material are set to follow the Maxwell-Boltzmann distribution of temperature T_H. The initial velocities of other atoms are zero. The velocities of atoms within 10 Å from the edge are reset at every step by the velocity scaling method to keep $T^* = T_H$. Figure 4 (b) shows the simulation results obtained by using the HC equation for the system with the same configuration as that of the MD simulation. Thermal diffusivity α is estimated by comparing the time evolution of the depth profile of the temperature solved by the MD method to the profile solved by the HC equation with a different α. The lines shown in Fig. 5 denote the results using the HC equation with $\alpha = 3.93 \times 10^{-7}$ m^2/s. The marks denote the results obtained by the MD simulation. Even though T_H is different, the depth profile obtained by the HC equation with constant $\alpha = 3.93 \times 10^{-7}$ m^2/s shows a good agreement with the result of the MD simulation.

Thermal diffusivity α can be converted to thermal conductivity λ by multiplying $\rho c = (3/2)k_B n$ where ρ is the mass density, c is the specific heat, n is the number density, and k_B is the Boltzmann constant. From the relation, the value of λ in our simulation is obtained to be 1.34 W/(m · K). The value is in good agreement with the literature value of amorphous carbon, which is 1.5 W/(m · K) at 273 K [10].

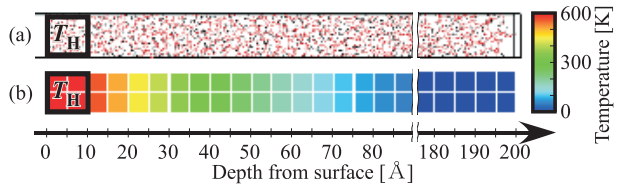

Fig. 4 Simulation of heat conduction using the (a) MD method and (b) HC equation.

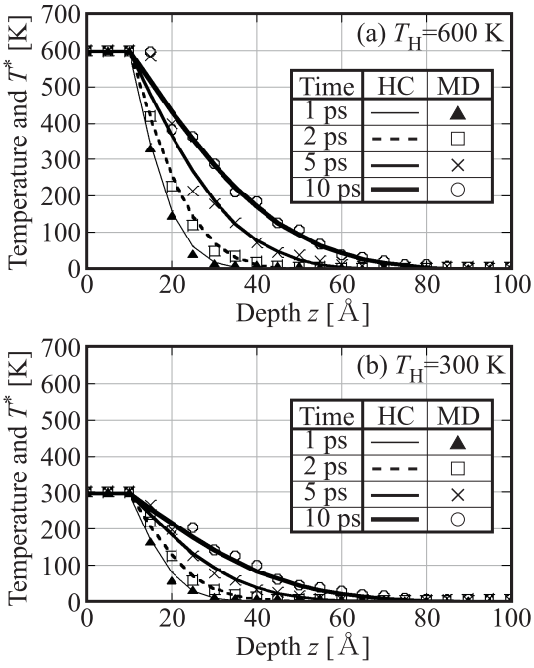

Fig. 5 Depth profile of temperature using the MD method and HC equation. The results obtained by solving the HC equation are the case where $\alpha = 3.93 \times 10^{-7}$ m^2/s.

3. Validation and Verification of the Model

3.1 Cell size dependence

To investigate the cell size dependence of the MD-HC hybrid simulation, we calculated the depth profile of the T_{cell} of the system shown in Fig. 4 by the MD-HC hybrid simulation. To apply the hybrid simulation for the system, the material shown in Fig. 4 (a) is cut at a depth of 50 Å. After some treatment stabilize of the material, the HC region with a different cell size L is connected to the material. The thickness of the connection cells is set to 10 Å. Figure 6 shows the cell size dependence of the depth profile of the T_{cell} of the system using by the hybrid simulation. A depth lower than 50 Å is calculated by MD, and the deeper region is solved by the HC equation. When the cell size L is larger than 2.5 Å, almost the same depth profile is obtained. In these cases, the depth profile at the interface between the MD region and the HC region is smoothly connected. However, when the cell size L is 1.25 Å, the profile does not smoothly connect at the interface because the fluctuation of T^* in each cell is large when the number of atoms in a cell is small. Therefore, the cell size L must be larger than 2.5 Å for the hybrid simulation.

3.2 MD region size dependence

To confirm the reliability of the MD-HC hybrid simulation, the time evolution of the radial distribution of T^* of the target material is compared by changing the size of the MD region without changing the size of the entire system composed of the HC region and the MD region. For the comparison, a larger material is prepared by repeating the structure of the original target material twice in the x-

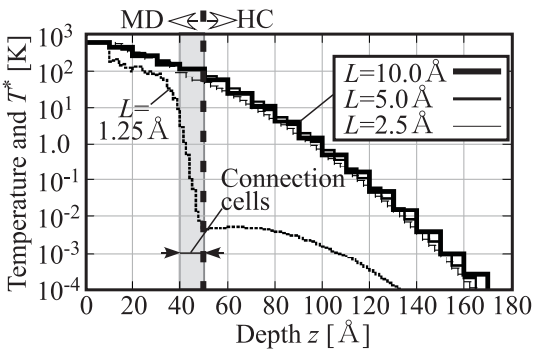

Fig. 6 Cell size dependence of the depth profile of T_{cell} calculated by the MD-HC hybrid simulation applied to the one-dimensional system shown in Fig. 4. T_H is set to 600 K. The profile is the value at the time of 10 ps.

and y-directions in addition to the original target material whose size is 40 Å × 40 Å × 33.3 Å. The size of the MD region of a larger case is 80 Å × 80 Å × 33.3 Å. The cell size of both the original and larger MD region case is set to 6.67 Å. The number of cells in the original and larger MD region case is $6 \times 6 \times 5$ and $12 \times 12 \times 5$, respectively. The HC region is attached around the MD region. The total number of cells, including both the HC and MD regions is $26 \times 26 \times 26$ for both original and larger MD region cases.

To calculate of the radial distribution of T^*, cylinders, which have the incident axis as its axis, are considered (as shown in Fig. 7). The radial distribution of T^* is calculated for every region between the cylinders whose radii are r and $r + \Delta r$. The value of Δr is set to 1 Å.

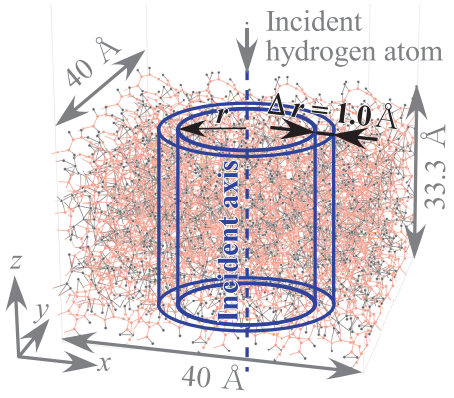

Fig. 7 Configuration of the cylinder for the calculation of the radial profile of T^* of the target material.

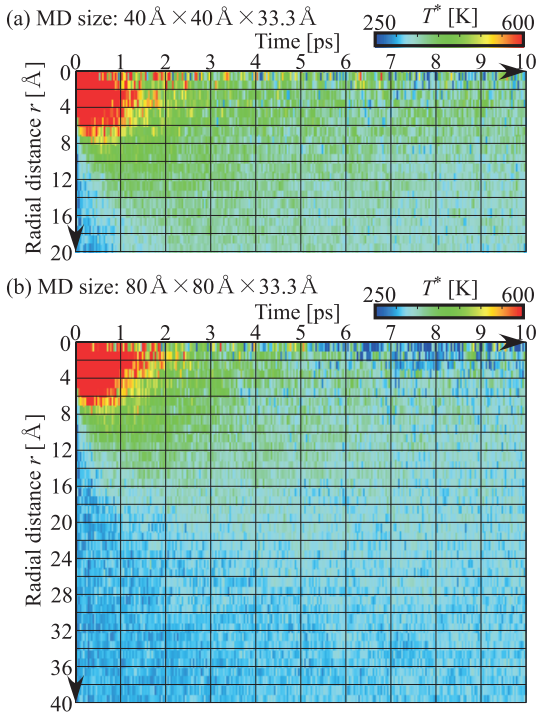

Fig. 8 Time evolution of the radial profile of T^* of the target material in the case where the size of the MD region is (a) 40 Å × 40 Å × 30 Å and (b) 80 Å × 80 Å × 30 Å.

Figure 8 shows the time evolution of the radial profile of T^* of the target material in the MD region for original and larger case. It is observed that the incident energy propagated toward the radial direction. Although it has already been shown in Fig. 11, after approximately 2 ps, the incident energy reached $r = 20$ Å where the connection cells are located in the original case. A decrease in the values of T^* near the center (i.e. $r < 10$ Å) is observed in both cases especially after 2 ps. Although the radial distributions of T^* in both cases are similar, we observe that the values of T^* near the center in the original case are slightly larger than those in the larger case when the time is more than 4 ps. It appears that this difference occurs because a part of the heat flow reaching the connection cells returns to the MD region through the periodic boundary. This returning energy can be reduced by increasing the size of the MD region. Therefore, it is necessary to determine the size of the MD region by considering the balance between computation cost and the amount of allowable returning energy.

3.3 Validation of thermal equilibrium in the connection cells

The process in which the incident atom collides with the surrounding atom in the target material and the incident energy is transferred to the surrounding atom is expected to be a non-equilibrium process. However, to connect the heat flow flowing out of the MD region to the HC equation, the atoms in the connection cells must be in a thermal equilibrium state. To validate the thermal equilibrium in the connection cells, the distributions of the kinetic energies of atoms in Cell-A and Cell-B, shown in Fig. 9, are investigated. Cell-A is located at the center of the target material where the incident atom penetrates. Cell-B is located in the connection cells which are shown as hatched cells in Fig. 9. Cell-A and Cell-B contain 41 and 44 atoms, respectively. To secure a sufficient sample size, the kinetic energy values for each atom in 100 steps (2 fs) is used for each plot. Therefore, the sample size for each plot is 4100

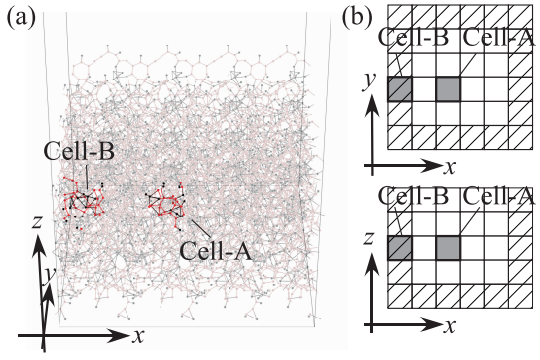

Fig. 9 (a) Atoms in Cell-A and Cell-B. (b) Positions of Cell-A and Cell-B.

and 4400 for Cell-A and Cell-B, respectively.

Figure 10 shows the time evolution of the distribution of kinetic energies of atoms in Cell-A and Cell-B. The solid red line shows the Maxwell-Boltzmann distribution where temperature T is equal to T^* of Cell-A or Cell-B. The energy distribution of Cell-A follows the Maxwell-Boltzmann distribution after 0.02 ps because the incident atom does not reach Cell-A yet. However, the distribution considerably deviates from the Maxwell-Boltzmann distribution after 0.04 ps because the incident atom collides with atoms in Cell-A. As time elapses, energy relaxation proceeds. After 1 ps, the distribution follows the Maxwell-Boltzmann distribution again even though T^* is still higher than the initial temperature. Compared with Cell-A, the distribution of Cell-B always follows the Maxwell-Boltzmann distribution even though T^* at 1 ps is higher than the initial temperature. Therefore, we conclude that the atoms in the connection cells are in a thermal equilibrium state.

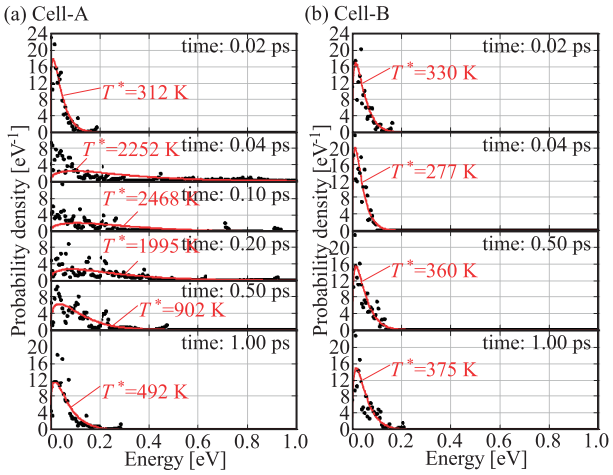

Fig. 10 Distribution of kinetic energies of atoms in (a) Cell-A and (b) Cell-B. Solid red line shows the maxwell distribution when the temperature is T^* of the cell.

4. Simulation Results and Discussion

Figure 11 shows the time evolution of the value of $T_{\rm cell}$ of each cell. Instead of temperature, the value of T^* is used for the cells in the MD region. After 7.2 fs, the incident atom is impacted at the center of the surface of the target material. Therefore, an increase in T^* is observed at the center after 0.1 ps. After 2 ps, the high energy area in the MD region expands. An increase in the temperature of the cells in the HC region adjacent to the MD region is also observed. After 10 ps, the area with an increased temperature in the HC region near the MD region expands. The values of T^* in the MD region gradually decreases. After 50 ps passed, the values of $T_{\rm cell}$ almost recover to the initial state.

Figure 12 shows the time evolution of the average kinetic energy T^* of the target material in the MD region. "The target material" includes all atoms in the MD region, excluding the incident atom. The dots are plotted

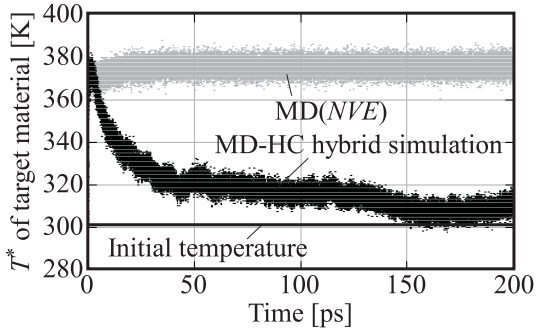

Fig. 12 Time evolution of the average kinetic energy T^* of the target material in the MD region. The black dots denote the results of the MD-HC hybrid simulation. The gray dots denote the results of the MD simulaitin under the NVE ensemble.

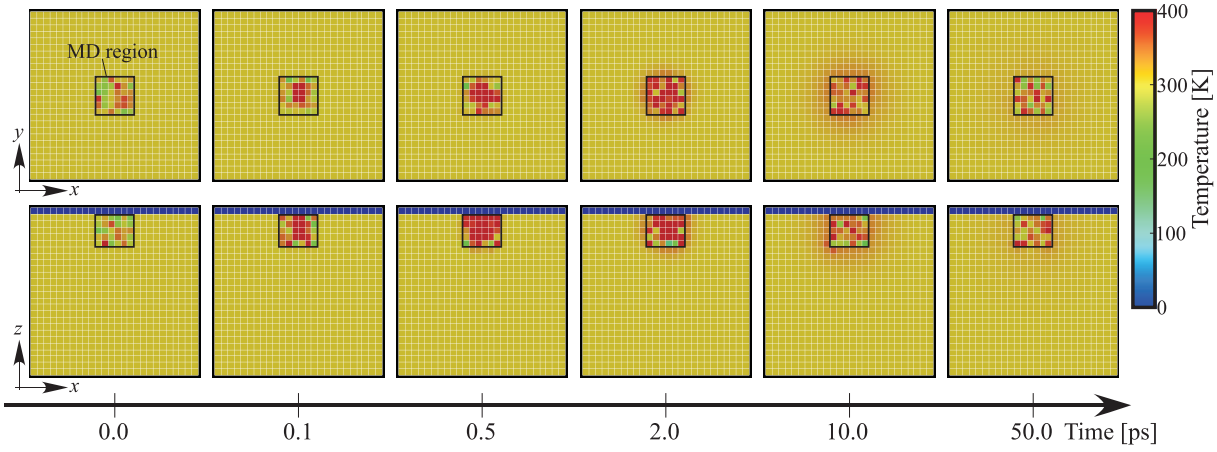

Fig. 11 Time evolution of the value of $T_{\rm cell}$ at each cell. Upper and lower figures show the cross-sectional schematic diagrams in x-y and x-z planes of the system of the MD-HC hybrid simulation, respectively.

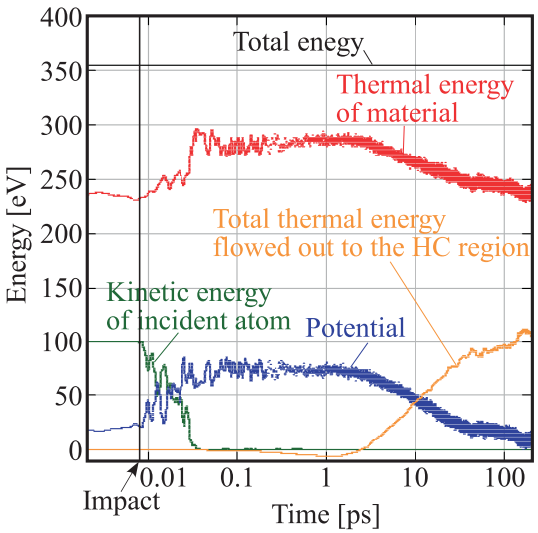

Fig. 13 Time evolution of energies in the MD region. The green line shows the kinetic energy of the incident atom. The red line shows the summation of kinetic energies of all atoms in the MD system except for the incident atom. The blue line shows the potential energy of all atoms in the MD system. The orange line shows the total energy removed from the MD system when energy is flowing out from the MD system.

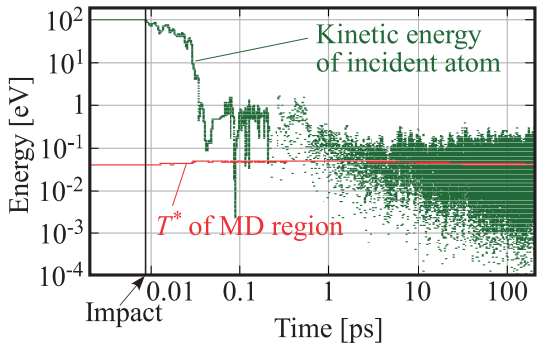

Fig. 14 Time evolution of kinetic energy of the incident atom (red line) and the average kinetic energy T^* of the MD region (green line).

every 2 fs. The black dots are calculated by the MD-HC hybrid simulation. The values increase to approximately 380 K from an initial temperature of 300 K when the incident atom enters the target material. Then, the values gradually decrease to recover the initial temperature owing to the heat flow from the MD region to the HC region. For the comparison, the result of a regular MD simulation under the *NVE* ensemble, which does not include the connection to the HC equation, is plotted as gray dots. In a regular MD simulation, the temperature does not return to the initial value. Of note, the computation times for 200 ps for the MD-HC hybrid simulation and regular MD simulation are 36349 s and 33721 s, respectively. Therefore, computation time increases by 7.8 %.

Figure 13 shows the time evolution of the kinetic energy of the incident atom, thermal energy of material, potential energy, and total thermal energy flowed out to the HC region. The dots are plotted every 0.02 fs when the time is less than 200 fs and every 2 fs when time is larger than 200 fs. The thermal energy of the material is calculated by adding the kinetic energies of all atoms in the target material. The total thermal energy flowed out to the HC region is calculated by summing up kinetic energies removed from the atoms in the connection cells using the velocity scaling method (i.e., step 9 explained in Sec. 2.2). Owing to the energy conservation law, the summation of all energies is conserved. After the impact, the kinetic energy of the incident atom gradually decreases by colliding with target atoms. Conversely, the thermal energy of target atoms and the potential energy increase with a decrease in the kinetic energy of the incident atom because the incident energy is transferred to the surrounding atoms in the target material. The energy absorption process occurs on a time scale of less than 0.1 ps. After 1 ps, the thermal energy of material and potential energy gradually decrease when the total thermal energy flowed out to the HC region increases. The heat removal process proceeds on a time scale of approximately 1000 times slower than the process of energy absorption process.

Figure 14 shows the time evolution of the kinetic energy of the incident atom and the average kinetic energy T^* of the target material in the MD region. For comparison, the value of T^* is plotted in the eV unit. Figure 14 clearly shows that the incident atom has the same energy as the surrounding atoms in the target material after approximately 1 ps.

5. Summary

A new calculation method is developed for the MD simulation of a system in which an atom is injected into a target material. In the new method, the boundary of the MD system is connected to the HC equation to consider the process of heat transfer of incident energy from the injection points to the bulk of the material. By applying the proposed method to the system of hydrogen atom injection into carbon material, we successfully simulated the process in which the incident energy propagated from the incident point to the surrounding atoms and recovered to the initial temperature with a small MD system. The simulation result shows that the process of heat removal proceeds on a time scale of approximately 1000 times slower than the time scale of when the incident energy transfers from the incident atom to the target material.

Acknowledgments

The research was partially supported by the Grant-in-Aid for Scientific Research, No.18K13528 and No.19K03800, from the Japan Society for the Promotion of Science, and by the NIFS Collaborative Research

Program NIFS16KOAP031.

[1] S.I. Krasheninnikov, A. Yu. Pigarov and D.J. Sigmar, Phys. Lett. A **214**, 285 (1996).
[2] K. Sawada and M. Goto, Atoms **4**, 29 (2016).
[3] M. Goto, K. Sawada, K. Fujii, M. Hasuo and S. Morita, Nucl. Fusion **51**, 023005 (2011).
[4] S. Saito, H. Nakamura, K. Sawada, G. Kawamura, M. Kobayashi and M. Hasuo, Contrib. Plasma Phys. e201900152 (2020).
[5] K. Sawada, H. Nakamura, S. Saito, G. Kawamura, M. Kobayashi, K. Haga, T. Sawada and M. Hasuo, Contrib. Plasma Phys. e201900153 (2020).
[6] S. Saito, A.M. Ito, A. Takayama and H. Nakamura, Jpn. J. Appl. **51**, 01AC05 (2012).
[7] J. Roth, E. Tsitrone, T. Loarer, V. Philipps, S. Brezinsek, A. Loarte, G.F. Counsell, R.P. Doerner, K. Schmid and O.V. Ogorodnikova, Plasma Phys. Control. Fusion **50**, 103001 (2008).
[8] D.W. Brenner, O.A. Shenderova, J.A. Harrison, S.J. Stuart, B. Ni and S.B. Sinnott, J. Phys.: Condens. Matter **14**, 783 (2002).
[9] M. Suzuki, J. Math. Phys. **26**, 601 (1985).
[10] National Astronomical Observatory of Japan, *Chronological Scientific Table* (Maruzen, 2000) p. 478.